Trends in Computational and Applied Mathematics, **26** (2025), e01839
Sociedade Brasileira de Matemática Aplicada e Computacional
Online version ISSN 2676-0029 www.scielo.br/tcam
ORIGINAL ARTICLE
doi: 10.5540/tcam.2025.026.e01839

An Application of Two Models for COVID-19 in Brazil

R. S. MARCOLINO[1*] and J.F.C.A. MEYER[2]

Received on November 21, 2024 / Accepted on June 15, 2025

ABSTRACT. This work involves the study and development of epidemiological models described through systems of evolutionary and nonlinear ordinary differential equations. Additionally, it includes case studies related to the dynamics of COVID-19. The proposed original models examine the impact of contingency measures and vaccination strategies on the social dynamics of infectious diseases. Finally, a comparative discussion is presented, analyzing the results of the proposed models and their computational simulations against real data collected in Brazil.

Keywords: COVID-19 - epidemiology, ordinary differential equations, mathematical modeling.

1 INTRODUCTION

Historical records reveal the greatest pandemic of antiquity: the Plague of Egypt. This pandemic occurred between 430 BC and 427 BC and, during the Peloponnesian War, decimated two-thirds of the population of Athens. Between the 2nd and 3rd centuries AD, two pandemics hit the Roman Empire: the Plague of Antoninus, around 165 AD, and the Plague of Cyprian, in 250 AD. This was followed by the so-called Black Death, which began in Central Asia in 1347 and became the largest and most devastating pandemic in history. Its effects altered the demographics of much of the world, killing young and old, men, women, and children in lethal ways [8].

The World Health Organization (WHO) declared COVID-19 a global pandemic in March 2020. This pandemic has disrupted activities across the world and forced many countries to reset their economies. Different control policies have been recommended by the WHO, such as lockdowns, quarantines, isolation, and social distancing. Unfortunately, these control measures have caused economic slowdowns, increased mortality, inflation, high crime rates, lawlessness, and famine in many countries [12].

After approximately three years of fighting the epidemic, and with the development and distribution of vaccines and medicines, the World Health Organization (WHO) declared the end of

*Corresponding author: R. S. Marcolino – E-mail: raimundo.marcolino@ifma.edu.br
[1]Federal Institute of Education, Science and Technology of Maranhão, Department of Mathematics, Poraquê Village, s/n, Rural Area, Codó, MA, Brazil — E-mail: raimundo.marcolino@ifma.edu.br https://orcid.org/0000-0002-2479-6811
[2]IMECC, University of Campinas, Department of Applied Mathematics, R. Sérgio Buarque de Holanda, 651, 13083-859, Campinas, SP, Brazil — E-mail: jmeyer@unicamp.br https://orcid.org/0000-0001-8002-7075

the Public Health Emergency of International Concern (PHEIC) related to COVID-19 in May 2023, in Geneva, Switzerland. This declaration was made after almost 700 million people had been infected and, at the time of writing, nearly 7 million people had died as a result of the disease [20].

The models are based on the SEAIR system and its extension with vaccination (SEAIRV). This approach considers temporary immunity, which distinguishes this work from other models that assume permanent immunity. The objective is to obtain theoretical and numerical results that not only contribute to the understanding of the social dynamics of diseases but also serve as a starting point for new studies in this necessary transdisciplinary field of research.

This study aims to illustrate possible scenarios for the evolution of COVID-19 in Brazil by applying a method implemented using Octave software. To this end, we numerically approximate the solution of the nonlinear system of differential equations and compare the results of our models with real-world data.

The structure of the paper is as follows: Section 2 presents two mathematical models of the types SEAIR (Susceptible – Exposed – Asymptomatic – Infectious – Recovered) and SEAIRV (Susceptible – Exposed – Asymptomatic – Infectious – Recognized – Vaccinated). In these models, we analyze the local stability of the disease-free equilibrium using the basic reproduction number $\mathscr{R}_0$. In Section 3, we present numerical simulations of the population in each compartment of the model presented in Section 2. Section 4 presents the results, including parameter estimation to compare the graphical simulations with real COVID-19 data from Brazil and the SEAIR and SEAIRV models. We conclude this work with Section 5, which provides our final considerations and suggestions for future research.

2 EPIDEMIOLOGICAL MATHEMATICAL MODELS

In line with more recent modeling approaches [1, 3, 15], the following work, although similar, represents an original contribution, with compartments comparable to those used in the cited studies. These include the traditionally used compartments: S (Susceptible), E (Exposed), A (Asymptomatic), I (Infected), and R (Recovered or Removed). Additionally, one more compartment is considered, which is also commonly used in many other models: V, representing vaccinated individuals.

2.1 SEAIR Mathematical Model

It is important to note that, although many other models consider the same or similar compartments, the models presented here exhibit unique and original features. The compartmental diagram for this model is shown in Figure 1.

The parameters of this model are as follows: β_1, the transition rate from S to E (transmission coefficient representing susceptible individuals becoming exposed, i.e., those who acquire the virus but are not yet infectious); α, the transition rate from E to I (rate at which exposed individuals

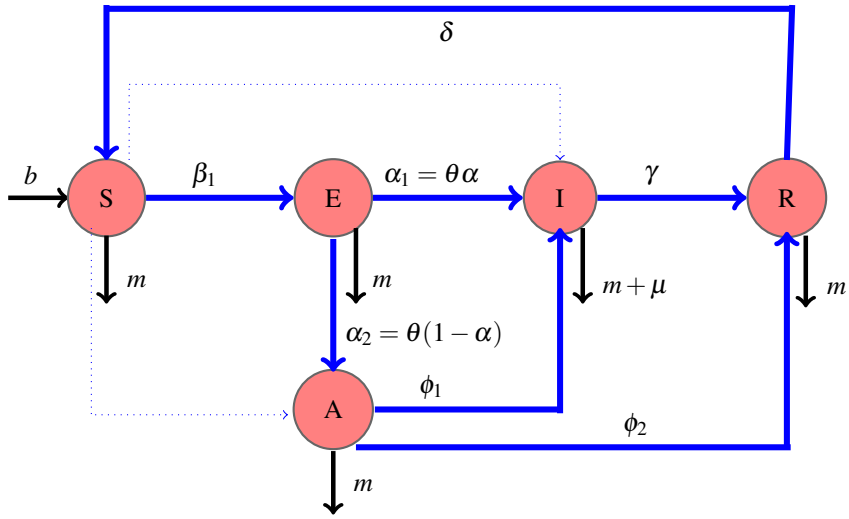

Figure 1: Compartmental diagram of the SEAIR model.
Source: Author.

develop symptoms at the end of the incubation period); γ, the recovery rate of individuals in compartment I; ϕ_1, the transition rate from A to I (rate at which asymptomatic individuals progress to the infectious compartment); ϕ_2, the recovery rate of individuals in compartment A; δ, the rate at which recovered individuals return to the susceptible class; θ, the incubation/latency rate; b, the birth rate; m, the natural mortality rate; and μ, the disease-induced mortality rate. All parameters are assumed to be positive.

The SEAIR model is described by the following system of differential equations:

$$\begin{cases} \frac{dS}{dt} &= bN + \delta R - \beta_1 SA/N - \beta_1 SI/N - mS \\ \frac{dE}{dt} &= \beta_1 SA/N + \beta_1 SI/N - (\alpha_1 + \alpha_2 + m)E \\ \frac{dA}{dt} &= \alpha_2 E - (\phi_1 + \phi_2 + m)A \\ \frac{dI}{dt} &= \alpha_1 E + \phi_1 A - (\gamma + \mu + m)I \\ \frac{dR}{dt} &= \phi_2 A + \gamma I - (\delta + m)R \end{cases}, \tag{2.1}$$

with $\alpha_1 = \theta\alpha$, $\alpha_2 = \theta(1-\alpha)$, $S(0) > 0$, $E(0) \geq 0$, $A(0) \geq 0$, $I(0) \geq 0$, $R(0) \geq 0$ [11].

Adding the equations of (2.1),we obtain the expression of the dynamics of the model for the population of individuals, therefore,

$$\frac{dN}{dt} = bN - mN - \mu I, \tag{2.2}$$

Since N is the total population, we have $N = S + E + A + I + R$, and in the absence of the disease, the model dynamics reduce to the expression,

$$\frac{dN}{dt} = N(b - m). \tag{2.3}$$

2.1.1 Basic Reproduction Number of the Model (2.1)

The basic reproduction number, denoted by $\mathscr{R}_0$, is the expected number of secondary cases produced by a single infectious individual in a completely susceptible population [4]. Therefore, the DFE (Disease-Free Equilibrium) is given by $(bN/m, 0, 0, 0, 0)$ and will be determined using the *Next Generation Matrix* (NGM) method, as introduced by Van den Driessche and Watmough [18]. We consider the vector $x = (E, A, I)$, since, when applying this method, one introduces the compartments responsible for the transmission of the disease or those that serve as links to a transmission compartment.

In the models, the population studied is considered constant ($b \cong m$), meaning it is always the sum of the populations in each compartment. A Malthusian population dynamic was adopted due to the relatively short study period.

Note that, in the study of model (2.1), there are three compartments to examine regarding disease transmission: E, A, and I. The latter two are associated with individuals who actively spread the disease. Although individuals in the E compartment do not transmit the disease, this compartment serves as a transition to the infectious compartments. Therefore, to analyze the disease-free equilibrium point, we consider $\bar{x}$ from the model and use the point $x = (E^*, A^*, I^*)$, focusing on the compartments that involve infection (exposed, asymptomatic, and infectious individuals). In the Next Generation Matrix (NGM) framework, $\mathscr{F}(x)$ denotes the rate of appearance of new infections in the transmission compartments; $\mathscr{V}^+(x)$ is the rate at which individuals enter the infectious compartments; and $\mathscr{V}^-(x)$ is the rate at which individuals leave the infectious compartments. Thus, $\mathscr{V}(x) = \mathscr{V}^-(x) - \mathscr{V}^+(x)$. Since $\dot{x}$ represents the derivatives of the vector x, we have $\dot{x} = f_i(x) = \mathscr{F}(x) - \mathscr{V}(x)$, and hence:

$$\mathscr{F}(x) = \begin{bmatrix} \beta_1 SA/N + \beta_1 SI/N \\ 0 \\ 0 \end{bmatrix},$$

$$\mathscr{V}^-(x) = \begin{bmatrix} (\alpha_1 + \alpha_2 + m)E \\ (\phi_1 + \phi_2 + m)A \\ (\gamma + \mu + m)I \end{bmatrix}, \quad \mathscr{V}^+(x) = \begin{bmatrix} 0 \\ \alpha_2 E \\ \alpha_1 E + \phi_1 A \end{bmatrix},$$

so that

$$\mathscr{V}(x) = \mathscr{V}^-(x) - \mathscr{V}^+(x) = \begin{bmatrix} (\alpha_1 + \alpha_2 + m)E \\ -\alpha_2 E + (\phi_1 + \phi_2 + m)A \\ -\alpha_1 E - \phi_1 A + (\gamma + \mu + m)I \end{bmatrix},$$

i.e.,

$$\dot{x} = f(x) = \mathscr{F}(x) - \mathscr{V}(x),$$

that is,

$$\begin{bmatrix} dE/dt \\ dA/dt \\ dI/dt \end{bmatrix} = \begin{bmatrix} \beta_1 SA/N + \beta_1 SI/N \\ 0 \\ 0 \end{bmatrix} - \begin{bmatrix} (\alpha_1 + \alpha_2 + m)E \\ -\alpha_2 E + (\phi_1 + \phi_2 + m)A \\ -\alpha_1 E - \phi_1 A + (\gamma + \mu + m)I \end{bmatrix}.$$

Applying the Jacobian to $\mathscr{F}(x)$ and $\mathscr{V}(x)$, we obtain:

$$D\mathscr{F}(x) = \begin{bmatrix} 0 & \beta_1 S/N & \beta_1 S/N \\ 0 & 0 & 0 \\ 0 & 0 & 0 \end{bmatrix},$$

$$D\mathscr{V}(x) = \begin{bmatrix} \alpha_1+\alpha_2+m & 0 & 0 \\ -\alpha_2 & \phi_1+\phi_2+m & 0 \\ -\alpha_1 & -\phi_1 & \gamma+\mu+m \end{bmatrix}.$$

Substituting the disease-free equilibrium $\bar{x} = x_0$ into $D\mathscr{F}(x)$ and $D\mathscr{V}(x)$ and assuming $b \cong m$, we obtain the Jacobian matrices evaluated at this point:

$$D\mathscr{F}(\bar{x}) = F(x_0) = \begin{bmatrix} 0 & \beta_1 & \beta_1 \\ 0 & 0 & 0 \\ 0 & 0 & 0 \end{bmatrix},$$

$$D\mathscr{V}(\bar{x}) = G(x_0) = \begin{bmatrix} \alpha_1+\alpha_2+m & 0 & 0 \\ -\alpha_2 & \phi_1+\phi_2+m & 0 \\ -\alpha_1 & -\phi_1 & \gamma+\mu+m \end{bmatrix},$$

thus,

$$F = \begin{bmatrix} 0 & \beta_1 & \beta_1 \\ 0 & 0 & 0 \\ 0 & 0 & 0 \end{bmatrix}, \quad G = \begin{bmatrix} \alpha_1+\alpha_2+m & 0 & 0 \\ -\alpha_2 & \phi_1+\phi_2+m & 0 \\ -\alpha_1 & -\phi_1 & \gamma+\mu+m \end{bmatrix},$$

and

$$G^{-1} = \begin{bmatrix} \frac{1}{\alpha_1+\alpha_2+m} & 0 & 0 \\ \frac{\alpha_2}{(\alpha_1+\alpha_2+m)(\phi_1+\phi_2+m)} & \frac{1}{\phi_1+\phi_2+m} & 0 \\ \frac{m\alpha_1+\alpha_1\phi_1+\alpha_2\phi_1+\alpha_1\phi_2}{(\gamma+\mu+m)(\alpha_1+\alpha_2+m)(\phi_1+\phi_2+m)} & \frac{\phi_1}{(\gamma+\mu+m)(\alpha_1+\alpha_2+m)} & \frac{1}{\gamma+\mu+m} \end{bmatrix}.$$

Hence,

$$FG^{-1} = \begin{bmatrix} \frac{\beta_1(m\alpha_1+\alpha_1\phi_1+\alpha_2\phi_1+\alpha_1\phi_2)+\beta_1\alpha_2(\gamma+\mu+m)}{(\gamma+\mu+m)(\alpha_1+\alpha_2+m)(\phi_1+\phi_2+m)} & \frac{\beta_1(\gamma+\mu+m)+\beta_1\phi_1}{(\gamma+\mu+m)(\phi_1+\phi_2+m)} & \frac{\beta_1}{\gamma+\mu+m} \\ 0 & 0 & 0 \\ 0 & 0 & 0 \end{bmatrix}.$$

The characteristic polynomial of the matrix FG^{-1} is given by:

$$\det[FG^{-1} - \lambda I] = 0 \Rightarrow$$

$$\det \begin{bmatrix} \frac{\beta_1(m\alpha_1+\alpha_1\phi_1+\alpha_2\phi_1+\alpha_1\phi_2)+\beta_1\alpha_2(\gamma+\mu+m)}{(\gamma+\mu+m)(\alpha_1+\alpha_2+m)(\phi_1+\phi_2+m)} - \lambda & \frac{\beta_1(\gamma+\mu+m)+\beta_1\phi_1}{(\gamma+\mu+m)(\phi_1+\phi_2+m)} & \frac{\beta_1}{\gamma+\mu+m} \\ 0 & -\lambda & 0 \\ 0 & 0 & -\lambda \end{bmatrix} = 0.$$

Therefore, the characteristic polynomial of FG^{-1} is:

$$p(\lambda) = \lambda^3 - \frac{\beta_1(m\alpha_1+\alpha_1\phi_1+\alpha_2\phi_1+\alpha_1\phi_2)+\beta_1\alpha_2(\gamma+\mu+m)}{(\gamma+\mu+m)(\alpha_1+\alpha_2+m)(\phi_1+\phi_2+m)}\lambda^2 = 0.$$

The eigenvalues are:

$$\lambda_1 = \frac{\beta_1(m\alpha_1+\alpha_1\phi_1+\alpha_2\phi_1+\alpha_1\phi_2)+\beta_1\alpha_2(\gamma+\mu+m)}{(\gamma+\mu+m)(\alpha_1+\alpha_2+m)(\phi_1+\phi_2+m)}, \quad \lambda_2 = 0, \quad \lambda_3 = 0.$$

Therefore, since λ_1 is the largest spectral radius of the matrix FG^{-1}, it follows that

$$\mathscr{R}_0 = \frac{\beta_1(m\alpha_1+\alpha_1\phi_1+\alpha_2\phi_1+\alpha_1\phi_2)+\beta_1\alpha_2(\gamma+\mu+m)}{(\gamma+\mu+m)(\alpha_1+\alpha_2+m)(\phi_1+\phi_2+m)}. \tag{2.4}$$

2.1.2 Stability Analysis of Model Equilibrium Points (2.1)

The stability analysis of the equilibrium points of model (2.1), whether disease-free or endemic, is quite stimulating and serves as an important tool for analysis in various models. For this analysis, we consider $b \cong m$ and determine the stationary points, which are found when all the derivatives of the system's equations are set to zero.

$$\begin{cases} bN+\delta R-\beta_1 SA/N-\beta_1 SI/N-mS &= 0 \\ \beta_1 SA/N+\beta_1 SI/N-(\alpha_1+\alpha_2+m)E &= 0 \\ \alpha_2 E-(\phi_1+\phi_2+m)A &= 0 \\ \alpha_1 E+\phi_1 A-(\gamma+\mu+m)I &= 0 \\ \phi_2 A+\gamma I-(\delta+m)R &= 0 \end{cases}. \tag{2.5}$$

Let (S^*,E^*,A^*,I^*,R^*) denote the disease-free equilibrium variables of system (2.1). We have $A^* = \frac{\alpha_2 E^*}{\phi_1+\phi_2+m}$, and if $E^* = 0$, then $\bar{x} = (N,0,0,0,0)$, where $S^* = \frac{bN}{m} = N$, which corresponds to the disease-free equilibrium point obtained from the system equations. Note that at point $\bar{x}$, all compartments associated with the disease are zero; therefore, we can state that the entire population is susceptible. For this reason, we refer to $\bar{x}$ as the disease-free equilibrium (DFE).

In the case that follows, the values are expressed as functions of the constant exposed population.

If $E \neq 0$, we have the following expressions:

By isolating $\bar{A}$ in the third equation of system (2.5), we obtain:

$$\bar{A} = \frac{\alpha_2 \bar{E}}{\phi_1+\phi_2+m}. \tag{2.6}$$

By isolating $\bar{I}$ in the fourth equation of system (2.5) and substituting expression (2.6), we find

$$\bar{I} = \frac{\alpha_1\bar{E}(\phi_1+\phi_2+m)+\phi_1\alpha_2\bar{E}}{(\phi_1+\phi_2+m)(\gamma+\mu+m)}. \tag{2.7}$$

By isolating $\bar{R}$ in the fifth equation of system (2.5) and substituting expressions (2.6) and (2.7), we obtain

$$\bar{R} = \frac{\gamma\alpha_1\bar{E}(\phi_1+\phi_2+m)+\gamma\phi_1\alpha_2\bar{E}+\phi_2\alpha_2\bar{E}(\gamma+\mu+m)}{(\delta+m)(\phi_1+\phi_2+m)(\gamma+\mu+m)}. \tag{2.8}$$

Finally, summing the first and second equations of system (2.5), isolating $\bar{S}$, and substituting expression (2.8), we have:

$$\bar{S} = \frac{bN}{m} + \frac{\delta\bar{E}[\gamma\alpha_1(\phi_1+\phi_2+m)+\gamma\phi_1\alpha_2+\phi_2\alpha_2(\gamma+\mu+m)]}{m(\phi_1+\phi_2+m)(\gamma+\mu+m)(\delta+m)} - \frac{(\alpha_1+\alpha_2+m)\bar{E}}{m}. \tag{2.9}$$

This corresponds to the endemic equilibrium point $\bar{P} = (\bar{S},\bar{E},\bar{A},\bar{I},\bar{R})$, and all its coordinates are expressed in terms of $\bar{E}$.

2.1.3 Disease Free Equilibrium Model (2.1)

The eigenvalues corresponding to the Jacobian matrix associated with system (2.1), computed at $\bar{x}$, determine the local stability of the disease-free equilibrium point. Thus, if the real parts of the roots of the characteristic equation $\det[J(\bar{x})-\lambda I]=0$ are negative, the equilibrium point is locally and asymptotically stable (LAS) [19], that is:

$$J(\bar{x}) = \begin{bmatrix} -m & 0 & -\beta_1 & -\beta_1 & \delta \\ 0 & -\alpha_1-\alpha_2-m & \beta_1 & \beta_1 & 0 \\ 0 & \alpha_2 & -\phi_1-\phi_2-m & 0 & 0 \\ 0 & \alpha_1 & \phi_1 & -\gamma-\mu-m & 0 \\ 0 & 0 & \phi_2 & \gamma & -\delta-m \end{bmatrix}$$

and

$$det[J(\bar{x})-\lambda I]=0 \Rightarrow$$

$$det\begin{bmatrix} -m-\lambda & 0 & -\beta_1 & -\beta_1 & \delta \\ 0 & -\alpha_1-\alpha_2-m-\lambda & \beta_1 & \beta_1 & 0 \\ 0 & \alpha_2 & -\phi_1-\phi_2-m-\lambda & 0 & 0 \\ 0 & \alpha_1 & \phi_1 & -\gamma-\mu-m-\lambda & 0 \\ 0 & 0 & \phi_2 & \gamma & -\delta-m-\lambda \end{bmatrix} = 0,$$

whose characteristic polynomial is

$$[(-m-\lambda)][-(\delta+m)-\lambda]P(\lambda)=0, \tag{2.10}$$

where the polynomial $P(\lambda)$ is given by

$$P(\lambda) = \lambda^3 + A\lambda^2 + B\lambda + C \tag{2.11}$$

with coefficients

$$A = \alpha_1+\alpha_2+\phi_1+\phi_2+\gamma+\mu+3m \tag{2.12}$$

$$B = (\alpha_1+\alpha_2+m)(\phi_1+\phi_2+m)+(\alpha_1+\alpha_2+m)(\gamma+\mu+m)+(\phi_1+\phi_2+m)(\gamma+\mu+m)- \alpha_1\beta_1-\alpha_2\beta_1 \tag{2.13}$$

$$C = (\alpha_1+\alpha_2+m)(\phi_1+\phi_2+m)(\gamma+\mu+m)-\alpha_2\beta_1(\gamma+\mu+m)-\beta_1(m\alpha_1+\alpha_1\phi_1+$$

$$\alpha_2\phi_1+\alpha_1\phi_2)=(\alpha_1+\alpha_2+m)(\phi_1+\phi_2+m)(\gamma+\mu+m)(1-\mathscr{R}_0). \tag{2.14}$$

The eigenvalues of (2.10) are $\lambda_1=-m$ and $\lambda_2=-(\delta+m)$. For the polynomial in (2.11), the remaining three eigenvalues, λ_3, λ_4, and λ_5, are obtained by finding the roots of the cubic equation, according to the Routh–Hurwitz criterion. For this analysis, the conditions are: $A>0$, $C>0$, and $AB>C$ [6].

- $A=\alpha_1+\alpha_2+\phi_1+\phi_2+\gamma+\mu+3m>0$, since according to model (2.1), all parameters are positive.
- $C=(\alpha_1+\alpha_2+m)(\phi_1+\phi_2+m)(\gamma+\mu+m)(1-\mathscr{R}_0)>0$, if and only if $\mathscr{R}_0<1$.
- It remains to show that $AB>C$, that is, $AB-C>0$. Thus:

$$[(\alpha_1+\alpha_2+m)+(\phi_1+\phi_2+m)+(\gamma+\mu+m)][(\alpha_1+\alpha_2+m)(\phi_1+\phi_2+m)+$$
$$(\alpha_1+\alpha_2+m)(\gamma+\mu+m)+(\phi_1+\phi_2+m)(\gamma+\mu+m)-\alpha_1\beta_1-\alpha_2\beta_1]-$$
$$[(\alpha_1+\alpha_2+m)(\phi_1+\phi_2+m)(\gamma+\mu+m)(1-\mathscr{R}_0)]>0,$$

if

$$2(\alpha_1+\alpha_2+m)(\phi_1+\phi_2+m)(\gamma+\mu+m)+(\alpha_1+\alpha_2+m)^2[(\phi_1+\phi_2+m)+(\gamma+\mu+m)]+$$
$$(\phi_1+\phi_2+m)^2[(\alpha_1+\alpha_2+m)+(\gamma+\mu+m)]+(\gamma+\mu+m)^2[(\alpha_1+\alpha_2+m)(\phi_1+\phi_2+m)]>$$

$\beta_1\alpha_1^2+\beta_1\alpha_2^2+2\beta_1\alpha_1\alpha_2+2\beta_1 m(\alpha_1+\alpha_2)+\beta_1\alpha_1(\gamma+\mu)+\beta_1\alpha_2\phi_2$. Therefore, under this condition:

I) If $\mathscr{R}_0<1$, then $C>0$, and since $A>0$ and $AB>C$, in this case we can conclude that $\bar{x}$ is a locally and asymptotically stable equilibrium point.

II) If $\mathscr{R}_0>1$, then $\bar{x}$ is an unstable equilibrium point.

2.1.4 Endemic equilibrium of the model (2.1)

We will study the possible existence and stability of endemic equilibria of model (2.1), that is, equilibria in which at least one of the infected components of the model is different from zero. The equilibrium point found is $\bar{P}=(\bar{S},\bar{E},\bar{A},\bar{I},\bar{R})$, with these elements appearing in expressions (2.6), (2.7), (2.8), and (2.9). We substitute expression (2.9) into the second equation of system (2.5) to obtain the expression for $\bar{E}$, considering $b\cong m$:

$$\delta\beta_1\left(\frac{\gamma\alpha_1 c+\gamma f+g e}{N m h c e}\right)\left(\frac{\alpha_1 c+\alpha_2 e+f}{c e}\right)\bar{E}^2-\frac{a\beta_1}{Nm}\left(\frac{\alpha_1 c+\alpha_2 e+f}{c e}\right)\bar{E}^2+$$
$$\left(\frac{\beta_1\alpha_1 c+\beta_1\alpha_2 c+\beta_1 f}{c e}-a\right)\bar{E}=0\Rightarrow$$

$$\left[-\frac{\beta_1(\alpha_1 ac+\alpha_2 ae+af)}{Nmce}+\left(\frac{\delta\gamma\alpha_1 c+\delta\gamma f+\delta ge}{Nmhce}\right)\left(\frac{\beta_1(\alpha_1 c+\alpha_2 e+f)}{ce}\right)\right]\bar{E}^2 + \left(\frac{\beta_1(\alpha_1 c+\alpha_2 e+f)-ace}{ce}\right)\bar{E}=0. \tag{2.15}$$

Where: $a=\alpha_1+\alpha_2+m$, $c=\phi_1+\phi_2+m$, $e=\gamma+\mu+m$, $f=\alpha_2\phi_1$, $g=\alpha_2\phi_2$, $h=\delta+m$.

The non-negative real solutions of equation (2.15) determine the equilibrium points of system (2.1). One of the roots is $\bar{E}=0$, since (2.15) is a quadratic equation with a zero constant term, and this root defines $\bar{x}$.

To verify the existence of the other solution, equation (2.15) was rewritten and solved as follows:

$$\bar{E}=\frac{Nmceh}{[aceh-\delta(\gamma\alpha_1 c+\gamma f+ge)]}\cdot\frac{1}{\mathscr{R}_0}(\mathscr{R}_0-1), \tag{2.16}$$

where $\mathscr{R}_0$ is defined in (2.4).

Assuming that $(a,c,e,h) > \delta(\gamma\alpha_1 c+\gamma f+g,e)$, we observe the following regarding the equilibrium point $\bar{P}$:

- If $\mathscr{R}_0<1$, then $\bar{E}<0$. In this case, the point $\bar{P}$ is not biologically meaningful, since $\bar{E}$ represents a subpopulation of individuals who have contracted the disease.
- Therefore, the necessary and sufficient condition for the existence and uniqueness of the endemic equilibrium $\bar{P}$ is that $\mathscr{R}_0>1$.

2.2 SEAIRV Mathematical Model

The same compartments and parameters from model (2.1) were used, with the addition of compartment V for vaccinated individuals and the parameters v and η, which represent, respectively, the vaccination rate and the vaccine efficacy. Here, we assume that vaccinated individuals are immune to the disease for a certain period, meaning that the immunity acquired through vaccination is temporary. After some time, they return to the susceptible class and can contract the disease again.

The diagram of this model is shown in Figure 2.

The system of equations for the SEAIRV model is given by (2.17).

$$\begin{cases} \frac{dS}{dt} &= bN+\delta R+\eta V-\beta_1 SA/N-\beta_1 SI/N-(v+m)S \\ \frac{dE}{dt} &= \beta_1 SA/N+\beta_1 SI/N-(\alpha_1+\alpha_2+m)E \\ \frac{dA}{dt} &= \alpha_2 E-(\phi_1+\phi_2+m)A \\ \frac{dI}{dt} &= \alpha_1 E+\phi_1 A-(\gamma+\mu+m)I \\ \frac{dR}{dt} &= \phi_2 A+\gamma I-(\delta+m)R \\ \frac{dV}{dt} &= vS-(\eta+m)V \end{cases}. \tag{2.17}$$

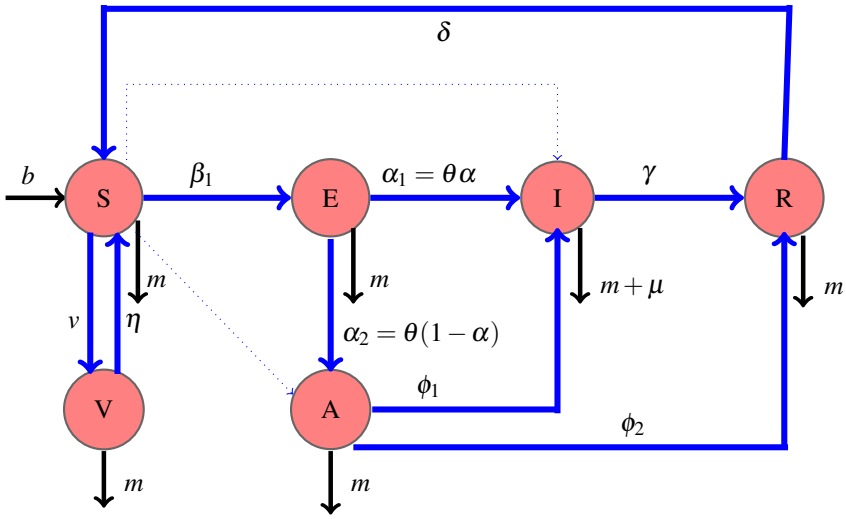

Figure 2: Compartmental diagram of the SEAIRV model.
Source: Author.

With $\alpha_1 = \theta\alpha$, $\alpha_2 = \theta(1-\alpha)$ and initial conditions $S(0) > 0$, $E(0) \geq 0$, $A(0) \geq 0$, $I(0) \geq 0$, $R(0) \geq 0$, and $V(0) \geq 0$, summing the equations in (2.17), we obtain the expression for the dynamics of the model in terms of the total population of individuals, namely:

$$\frac{dN}{dt} = bN - mN - \mu I, \tag{2.18}$$

where N is the total population, that is, $N = S + E + A + I + R + V$. If there is no disease, the expression for the model dynamics reduces to:

$$\frac{dN}{dt} = N(b-m). \tag{2.19}$$

2.2.1 Basic Reproduction Number of the Model (2.17)

We follow the same procedures as in model (2.1) [18], with the DFE given by the following expression:

$$\bar{x}_1 = \left(\frac{bN(\eta+m)}{(v+m)(\eta+m)-\eta v}, 0, 0, 0, 0, \frac{bvN}{(v+m)(\eta+m)-\eta v} \right).$$

Therefore, to compute $\mathscr{R}_0^V$, we use the NGM (Next Generation Matrix), that is, $\dot{x} = f_i(x) = \mathscr{F}(x) - \mathscr{V}(x)$, thus

$$\mathscr{F}(x) = \begin{bmatrix} \beta_1 SA/N + \beta_1 SI/N \\ 0 \\ 0 \end{bmatrix},$$

$$\mathscr{V}^-(x) = \begin{bmatrix} (\alpha_1+\alpha_2+m)E \\ (\phi_1+\phi_2+m)A \\ (\gamma+\mu+m)I \end{bmatrix}, \mathscr{V}^+(x) = \begin{bmatrix} 0 \\ \alpha_2 E \\ \alpha_1 E + \phi_1 A \end{bmatrix},$$

$$\mathscr{V}(x) = \mathscr{V}^-(x) - \mathscr{V}^+(x) = \begin{bmatrix} (\alpha_1+\alpha_1+m)E \\ -\alpha_2 E + (\phi_1+\phi_2+m)A \\ -\alpha_1 E - \phi_1 A + (\gamma+\mu+m)I \end{bmatrix},$$

that is

$$\dot{x} = f(x) = \mathscr{F}(x) - \mathscr{V}(x)$$

$$\begin{bmatrix} dE/dt \\ dA/dt \\ dI/dt \end{bmatrix} = \begin{bmatrix} \beta_1 SA/N + \beta_1 SI/N \\ 0 \\ 0 \end{bmatrix} - \begin{bmatrix} (\alpha_1+\alpha_2+m)E \\ -\alpha_2 E + (\phi_1+\phi_2+m)A \\ -\alpha_1 E - \phi_1 A + (\gamma+\mu+m)I \end{bmatrix}.$$

Applying the Jacobian to $\mathscr{F}(x)$ and $\mathscr{V}(x)$, we obtain

$$D\mathscr{F} = \begin{bmatrix} 0 & \beta_1 S/N & \beta_1 S/N \\ 0 & 0 & 0 \\ 0 & 0 & 0 \end{bmatrix}, D\mathscr{V} = \begin{bmatrix} \alpha_1+\alpha_1+m & 0 & 0 \\ -\alpha_2 & \phi_1+\phi_2+m & 0 \\ -\alpha_1 & -\phi_1 & \gamma+\mu+m \end{bmatrix}.$$

By substituting the disease-free equilibrium $\bar{x}_1 = x_0$ into $D\mathscr{F}(x)$ and $D\mathscr{V}(x)$, we find the Jacobian matrix evaluated at that point

$$D\mathscr{F}(\bar{x}_1) = F(x_0) =$$

$$\begin{bmatrix} 0 & \beta_1 b(\eta+m)/[(v+m)(\eta+m)-\eta v] & \beta_1 b(\eta+m)/[(v+m)(\eta+m)-\eta v] \\ 0 & 0 & 0 \\ 0 & 0 & 0 \end{bmatrix},$$

$$D\mathscr{V}(\bar{x}_1) = G(x_0) = \begin{bmatrix} \alpha_1+\alpha_2+m & 0 & 0 \\ -\alpha_2 & \phi_1+\phi_2+m & 0 \\ -\alpha_1 & -\phi_1 & \gamma+\mu+m \end{bmatrix},$$

therefore,

$$F = \begin{bmatrix} 0 & \frac{\beta_1 b(\eta+m)}{(v+m)(\eta+m)-\eta v} & \frac{\beta_1 b(\eta+m)}{(v+m)(\eta+m)-\eta v} \\ 0 & 0 & 0 \\ 0 & 0 & 0 \end{bmatrix},$$

$$G = \begin{bmatrix} \alpha_1+\alpha_2+m & 0 & 0 \\ -\alpha_2 & \phi_1+\phi_2+m & 0 \\ -\alpha_1 & -\phi_1 & \gamma+\mu+m \end{bmatrix},$$

and

$$G^{-1} = \begin{bmatrix} \frac{1}{\alpha_1+\alpha_2+m} & 0 & 0 \\ \frac{\alpha_2}{(\alpha_1+\alpha_2+m)(\phi_1+\phi_2+m)} & \frac{1}{\phi_1+\phi_2+m} & 0 \\ \frac{m\alpha_1+\alpha_1\phi_1+\alpha_2\phi_1+\alpha_1\phi_2}{(\gamma+\mu+m)(\alpha_1+\alpha_2+m)(\phi_1+\phi_2+m)} & \frac{\phi_1}{(\gamma+\mu+m)(\alpha_1+\alpha_2+m)} & \frac{1}{\gamma+\mu+m} \end{bmatrix}.$$

Then,

$$FG^{-1} = \begin{bmatrix} a_1 & a_2 & a_3 \\ 0 & 0 & 0 \\ 0 & 0 & 0 \end{bmatrix},$$

where

$$a_1 = \frac{b(\eta+m)\beta_1(m\alpha_1+\alpha_1\phi_1+\alpha_2\phi_1+\alpha_1\phi_2)+b(\eta+m)\beta_1\alpha_2(\gamma+\mu+m)}{[(\eta+m)(v+m)-\eta v](\gamma+\mu+m)(\alpha_1+\alpha_2+m)(\phi_1+\phi_2+m)},$$

$$a_2 = \frac{b(\eta+m)\beta_1(\gamma+\mu+m)+b(\eta+m)\beta_1\phi_1}{[(\eta+m)(v+m)-\eta v](\gamma+\mu+m)(\phi_1+\phi_2+m)},$$

and

$$a_3 = \frac{b(\eta+m)\beta_1}{[(\eta+m)(v+m)-\eta v](\gamma+\mu+m)}.$$

The characteristic equation of $\det(FG^{-1}-\lambda I)=0$ is

$$P(\lambda) = \lambda^2(a_1-\lambda) = 0,$$

thus, the roots of this equation are $\lambda_1 = a_1$, $\lambda_2 = 0$, and $\lambda_3 = 0$. Since

$$a_1 = \frac{b(\eta+m)\beta_1(m\alpha_1+\alpha_1\phi_1+\alpha_2\phi_1+\alpha_1\phi_2)+b(\eta+m)\beta_1\alpha_2(\gamma+\mu+m)}{[(\eta+m)(v+m)-\eta v](\gamma+\mu+m)(\alpha_1+\alpha_2+m)(\phi_1+\phi_2+m)}$$

is the spectral radius, then

$$\mathscr{R}_0^V = \frac{b(\eta+m)\beta_1(m\alpha_1+\alpha_1\phi_1+\alpha_2\phi_1+\alpha_1\phi_2)+b(\eta+m)\beta_1\alpha_2(\gamma+\mu+m)}{[(\eta+m)(v+m)-\eta v](\gamma+\mu+m)(\alpha_1+\alpha_2+m)(\phi_1+\phi_2+m)}. \tag{2.20}$$

The analysis of the inclusion of the expression $(v+m)(\eta+m)-\eta v$ can be carried out through successive numerical simulations using the Octave software, with a wide range of input data and parameters. This approach allows for the identification of different scenarios for the adopted models.

The analysis and stability of the SEAIRV model follow the same procedures and yield the same results as the SEAIR model, with the addition of the V (vaccinated) compartment.

3 NUMERICAL SIMULATIONS OF THE SEAIR AND SEAIRV MODELS

The method provided by the Octave *software* was used to numerically approximate the solutions of the nonlinear systems of differential equations (2.1) and (2.17). The algorithm implemented in Octave follows the Dormand-Prince method, one of the Runge-Kutta methods [14], performing six calculations per time step with a tolerance criterion corresponding to a precision of 0.0001%. This procedure minimizes the fifth- and sixth-order errors, respectively.

The purpose of presenting these results here was, of course, to numerically verify potential characterizations of endemic steady states. With the chosen parameters, it was possible to obtain outputs for values of $\mathscr{R}_0$ that are less than, equal to, and greater than one. It is clear that this numerical investigation does not constitute a formal proof of the stability of the obtained equilibrium points, but it does allow us to observe the behavior of the dependent variables, as illustrated in the graphs.

The parameters and initial conditions shown in Figures 3, 4, 5, and 6, although analogous and similar to those used in works such as [13, 14, 16], were specifically estimated for conducting the simulations of the two models presented here, namely: $\beta_1 = 0.085$, $\alpha_1 = \theta\alpha = 0.00204$, $\alpha_2 = \theta(1-\alpha) = 0.002796$, $\gamma = 0.005$, $\phi_1 = 0.0011$, $\phi_2 = 0.0042$, $\delta = 0.0035$, $v = 0.013$, $\eta =$

0.002, $b = 0.00035$, $m = 0.00035$, $\mu = 0.00050$, and for the initial conditions: $S = 500$, $E = 2$, $A = I = R = V = 0$. We chose to initialize the model with only susceptible individuals and a few exposed to the virus, representing those who initiate the presence of the disease within the population. This setup reflects the conditions observed at the onset of an epidemic, such as the emergence of COVID-19 in Brazil, as described in [2].

In Figure 3, one can observe the presence of an endemic equilibrium, as the disease does not vanish at any point. In this case, the system reaches a steady state (for the given parameters) after approximately 3.500 and 4.000 time steps in the models without and with vaccination, respectively.

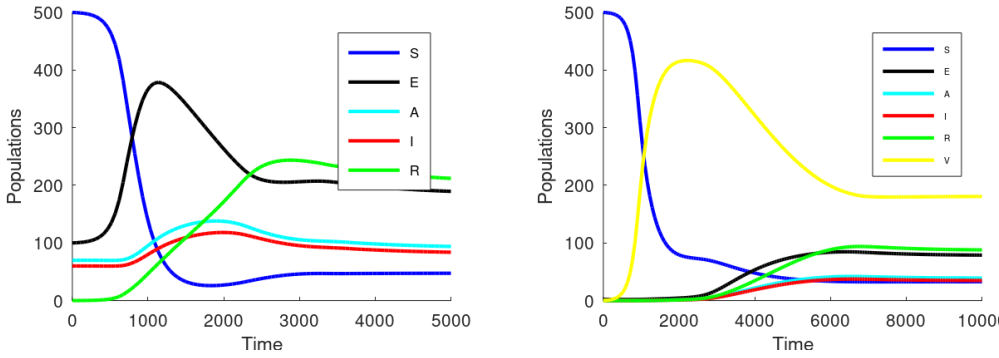

Figure 3: Graphical comparison of models (2.1) and (2.17).

Figure 4 applies the return rates δ and η of recovered and vaccinated individuals to the susceptible class, and it is observed that vaccination indeed affects the population by reducing the number of infected individuals compared to the scenario in which no vaccine is used.

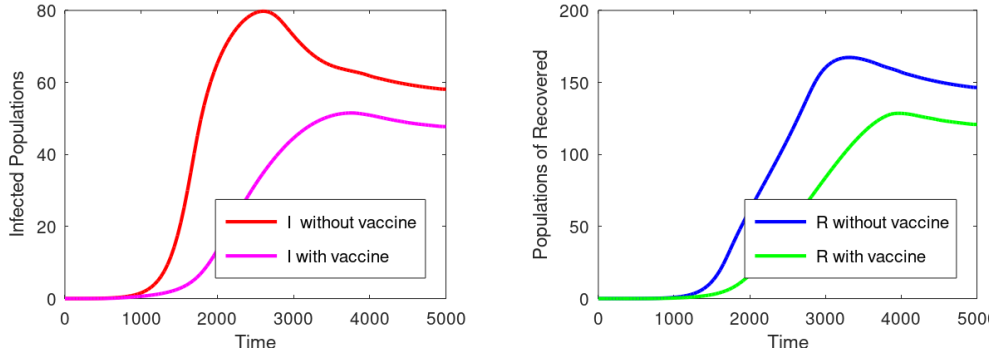

Figure 4: Comparison of the number of infected and recovered.

In Figure 5, we investigate how the transition from a stable disease-free equilibrium to an unstable one occurs as the basic reproduction number increases. A bifurcation can be described by a

graph of the equilibrium infectious population size, $\bar{I}$, as a function of the basic reproduction number $\mathscr{R}_0$ [5]. Therefore, we present the population of infected individuals at equilibrium, $\bar{I}$, as a function of $\mathscr{R}_0$ and $\mathscr{R}_0^V$, respectively. It is observed that as long as $\mathscr{R}_0 < 1$ and $\mathscr{R}_0^V < 1$, the only existing equilibrium is the disease-free one. However, when $\mathscr{R}_0$ and $\mathscr{R}_0^V$ increase to 1, a stability exchange occurs between the disease-free equilibrium and the endemic equilibrium (note that the endemic equilibrium is negative and unstable thus biologically meaninglessif $\mathscr{R}_0 < 1$ and $\mathscr{R}_0^V < 1$).

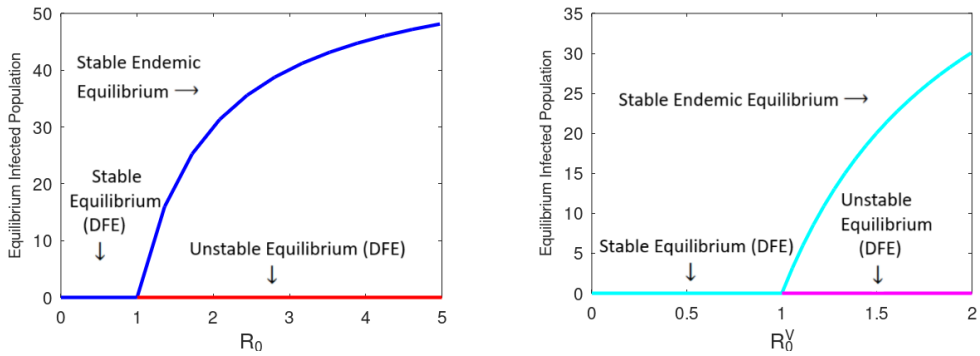

Figure 5: Forward bifurcation diagram of models (2.1) and (2.17).

Figure 6 shows the bifurcation diagram of the number of infected individuals as a function of the transmission rate. The expression for the number of infected individuals (2.7) was used, with the final result obtained by substituting expression (2.16), where $\mathscr{R}_0$ and $\mathscr{R}_0^V$ correspond to models (2.1) and (2.17), respectively. The resulting expressions are: $I(\beta)=60.241579761707065-60.241579761707065\times 0.00553683\beta^{-1}$ and $I(\beta_V)=60.241579761707065-60.241579761707065\times 0.036166096958878104\beta_V^{-1}$.

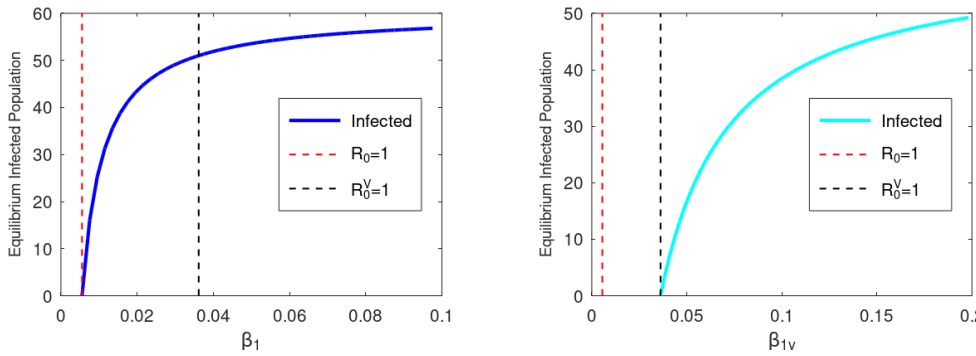

Figure 6: Bifurcation of, I, as a function of, β_1 of the models (2.1) and (2.17).

In this scenario, two dashed lines are illustrated: the red dashed line represents $\mathscr{R}_0 = 1$, and the black dashed line represents $\mathscr{R}0^V = 1$. It is observed that $\beta_1 < \beta 1v$ for $\mathscr{R}_0 = \mathscr{R}_0^V = 1$, which

implies that $\mathscr{R}_0 > \mathscr{R}0^V$ when $\beta_1 = \beta 1v$. This indicates that the vaccination policy indeed impacts the population by reducing the number of infected individuals when a vaccine is used.

4 NUMERICAL RESULTS WITH REAL DATA

We present a simulation of a scenario to compare the results of our models with real-world data on active COVID-19 cases in Brazil. In the simulation presented below, we also used the method provided by the Octave *software* to numerically approximate the solutions of the nonlinear systems of differential equations (2.1) and (2.17). To run the models, we used parameter values estimated from external sources, including scientific articles and real-world data.

The period considered in this scenario was from November 7, 2022, to February 26, 2023. For both models, the following initial conditions were established: $S(0) = 211426268$, $S_V(0) = 211300336$, $E(0) = 1650000$, $A(0) = 100000$, $I(0) = 123307$, $R(0) = 18064$, $V(0) = 125932$.

It is worth noting that the values for infected individuals (I) and recovered individuals (R) were obtained from [20], while the number of vaccinated individuals (V) was taken from [17]. The initial values for the exposed (E) and asymptomatic (A) populations were randomly assigned to reflect the scenario under consideration. The susceptible population (S) was calculated by subtracting the sum of the other compartment values from the total population of Brazil [10].

To obtain consistent estimates for the unknown parameters, the solutions were fitted to the available data from [17, 20] using the Octave *software*.

The parameter values and their respective sources are listed in Table 1.

Table 1: Parameter Values.

Parameters	Adopted Values	Likely Range (references)
α	0.65 day^{-1}	0.45 day^{-1} [2], 0.65 day^{-1} [14]
θ	$1/6$ day^{-1}	$1/6$ day^{-1} [11]
α_1	0.108	**Calculated from the values of α e θ**
α_2	0.058	**Calculated from the values of α e θ**
ϕ_1	$1/5$ day^{-1}	$1/5$ day^{-1} [20]
γ	$1/7$ day^{-1}	$1/3$ day^{-1} [2], $1/7$ day^{-1} [11]
ϕ_2	$1/10$ day^{-1}	$1/7$ day^{-1} [11], $1/14$ day^{-1} [2]
δ	$1/50$ day^{-1}	$1/50$ day^{-1} [14]
η	$1/180$ day^{-1}	$1/180$ day^{-1} [7]
m	$1/28105$ day^{-1}	$1/28105$ day^{-1} [9]

This scenario was generated using data from [17, 20] and the SEAIR and SEAIRV models, presented with the following parameters: $\beta_1 = 0.11$, tentatively assumed; $\mu = 0.0000114$ and $v = 0.00309$, taken from [20] and [17], respectively, as shown in Table 1. The estimated basic reproduction number is $\mathscr{R}_0 = 0.841$, and the vaccinated reproduction number is $\mathscr{R}_0^V = 0.541$, indicating a declining disease peak.

Figure 7 presents a comparison between the collected data on active cases and the proposed models, aiming to assess the differences between them. The results highlight the potential benefits of consistent vaccination programs in controlling the COVID-19 pandemic (and, more broadly, any epidemic or outbreak). What is identified here, from a public health perspective, as consistent vaccination—reflected in the difference in active cases between the SEAIR and SEAIRV models—proves to be highly significant under a systematic vaccination strategy over the studied period.

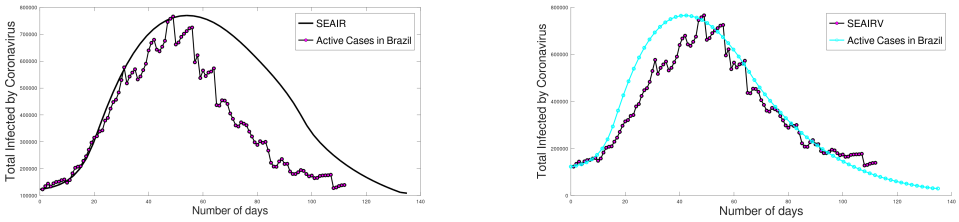

Figure 7: Active cases of the number of infected individuals in Brazil and the models (2.1) SEAIR e (2.17) SEAIRV.

Figure 8 presents a comparison between the two models and the active COVID-19 cases. It is observed that the model with vaccination (2.17), the SEAIRV model, closely resembles the real cases, as the analyzed period already included the vaccination campaign. In contrast, the model without vaccination shows a much higher disease peak compared to the actual active cases. This highlights the importance of vaccination campaigns in controlling and potentially eradicating the disease.

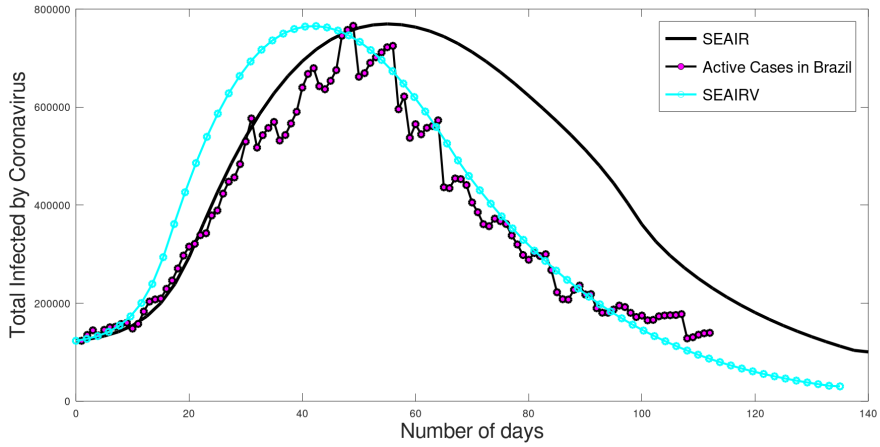

Figure 8: Active cases of the number of infected people in Brazil and the two models.

Figure 9 presents the phase plane for susceptible and infected individuals, highlighting the differences between the SEAIR and SEAIRV models. The figure also illustrates—albeit less prominently—the importance of vaccination strategies, as identified in this study, through the implementation of consistent vaccination programs.

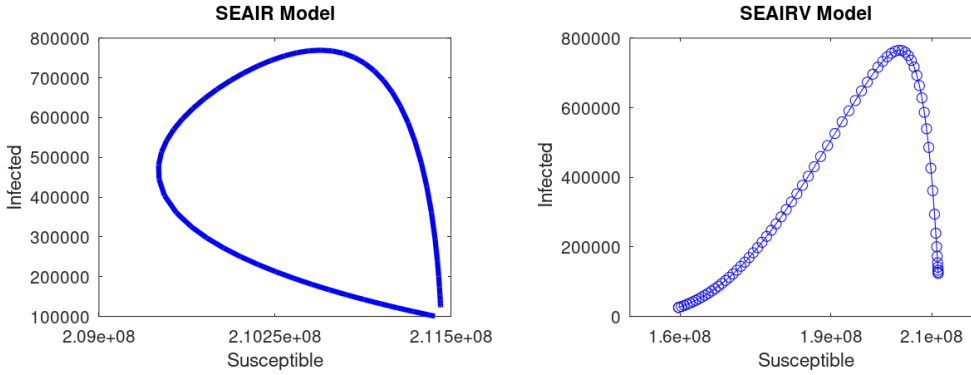

Figure 9: Simultaneous simulation of susceptible and infected individuals in Brazil.

Figure 10 shows a graphical comparison of the models with and without vaccination, considering varying values of the transmission rate (β_1). The figure depicts the evolution of infected individuals in the Brazilian population, revealing that an increase in the transmission rate leads to a higher number of infections. In both scenarios, it is evident how vaccination policy can impact the population by reducing the number of infected individuals compared to the situation where no vaccine is used.

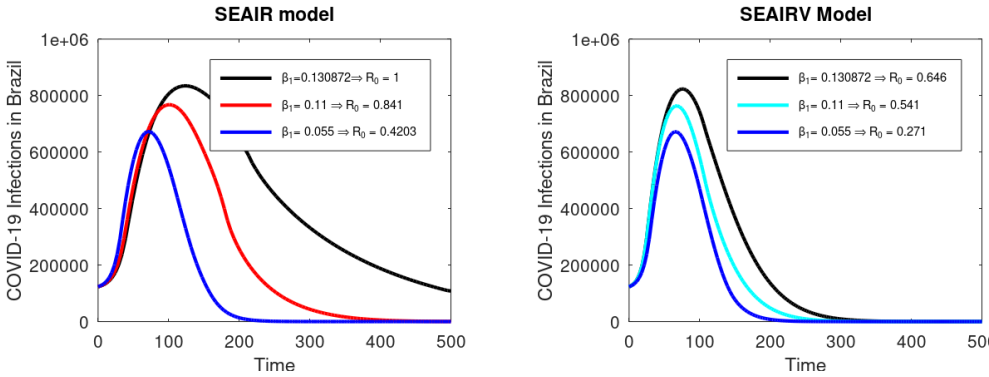

Figure 10: Comparison between models (2.1) and (2.17).

4.1 Discussion

From Figure 8, it is clear that mathematical modeling in epidemiology can be used to simulate evaluation scenarios for immunization programs and public health responses in the event of

epidemics and outbreaks. The close alignment between the SEAIRV model simulations and the actual pandemic situation in Brazil during the analyzed period, based on the collected data, highlights the importance of scientifically developed models in preparing society to face an epidemic or outbreak. These models could also serve as an early warning system when available vaccines are no longer administered for reasons unjustified from a scientific standpoint.

Therefore, in the presented scenario, the number of infected individuals decreases throughout Brazil, and the basic reproduction number remains below 1. It is worth noting that the models presented do not necessarily capture all factors involved in the disease but rather represent a starting point for a more detailed and structured study.

5 CONCLUSIONS

The main objective of this work was to develop two mathematical models to assess various epidemic and endemic scenarios, as well as the possible effects of mitigation, prevention, and, above all, immunization strategies. The models, which incorporate original aspects, were primarily based on observations of actions taken (or not taken) by federal, state, regional, and local public health authorities in response to the COVID-19 pandemic. It was the numerical data from this disease and its progression that informed the parameter values used to validate the models.

Numerical simulations were carried out using real-world data. In fact, these simulations demonstrated a decrease in the number of infected individuals, which can be attributed to isolation campaigns and the presumed temporary immunity provided by vaccination. Through this analytical effort, we have developed a numerical-computational tool that can be used to test public health strategies. With this tool, it would be possible to estimate potential effects prior to their implementation in society, particularly among high-risk populations. It could also serve as an initial approach to evaluating the risks associated with disregarding science and its contributions.

Finally, we believe that future work could involve the development of models that take into account differences in population composition and responses to social distancing, as the integration of real-time data could improve the accuracy of predictions and enable dynamic adjustments to the models. Therefore, it is important to emphasize that the two models presented here do not necessarily represent all factors involved in the disease but should rather be seen as a starting point for a more comprehensive and structured study aimed at contributing to the eradication of COVID-19.

Data availability

The data that support the findings of this study are available at `http://www.worldometers.info/coronavirus/country/brazil/andhttps://infoms.saude.gov.br/extensions/SEIDIGI_DEMAS_Vacina_C19/SEIDIGI_DEMAS_Vacina_C19.html`.

Associate editor: Rosana Sueli Motta Jafelice

REFERENCES

[1] H.A. Adekola, I.A. Adekunle, H.O. Egberongbe, S.A. Onitilo & I.N. Abdullahi. Mathematical modeling for infectious viral disease: The COVID-19 perspective. *Journal of public affairs*, **20**(4) (2020), e2306.

[2] M. Amaku, D.T. Covas, F.A.B. Coutinho, R.S. Azevedo & E. Massad. Modelling the impact of contact tracing of symptomatic individuals on the COVID-19 epidemic. *Clinics*, **76** (2021).

[3] O. Diallo, Y. Kone, C. Sanogo *et al.* A mathematical model of COVID-19: Analysis and identification of parameters for better decision making. *Applied Mathematics*, **13**(2) (2022), 205–214.

[4] O. Diekmann, J.A.P. Heesterbeek & J.A. Metz. On the definition and the computation of the basic reproduction ratio R_0 in models for infectious diseases in heterogeneous populations. *Journal of mathematical biology*, **28**(4) (1990), 365–382.

[5] J. Dushoff, W. Huang & C. Castillo-Chavez. Backwards bifurcations and catastrophe in simple models of fatal diseases. *Journal of mathematical biology*, **36** (1998), 227–248.

[6] L. Edelstein-Keshet. "Mathematical models in biology". SIAM (2005).

[7] D.R. Feikin, M.M. Higdon, L.J. Abu-Raddad, N. Andrews, R. Araos, Y. Goldberg, M.J. Groome, A. Huppert, K.L. O'Brien, P.G. Smith *et al.* Duration of effectiveness of vaccines against SARS-COV-2 infection and COVID-19 disease: results of a systematic review and meta-regression. *The Lancet*, (2022).

[8] A.C. Fernandes *et al.* As grandes pandemias da história da Europa e os seus impactos na nossa civilização: desafios da moderna saúde pública. *Cadernos Ibero-Americanos de Direito Sanitário*, **10**(2) (2021), 19–30.

[9] IBGE. Instituto Brasileiro de Geografia e Estatística, Estimativa da expectativa de vida da população brasileira (2021). URL `https://www.ibge.gov.br/novo-portal-destaques.html?destaque=35600`. Acessado em 21/02/2023.

[10] IBGE. Instituto Brasileiro de Geografia e Estatística, Estimativa da Polpulação Brasileira (2021). URL `https://www.ibge.gov.br/estatisticas/sociais/populacao/9103-estimativas-de-populacao.html?=&t=resultados`. Acessado 02/03/2023.

[11] E. Iboi, O.O. Sharomi, C. Ngonghala & A.B. Gumel. Mathematical modeling and analysis of COVID-19 pandemic in Nigeria. *MedRxiv*, (2020).

[12] C.E. Madubueze, N.M. Akabuike & S. Dachollom. The role of mathematical model in curbing COVID-19 in Nigeria. *medRxiv*, **3** (2020), 135–147.

[13] J. Meyer & M. Lima. Relevant mathematical modelling efforts for understanding COVID-19 dynamics: An educational challenge. *ZDM–Mathematics Education*, **55**(1) (2023), 49–63.

[14] J. Meyer, M. Lima, C. Espitia, F. Longo, B. Laiate, A. Gois & C. Kunz. Different Approaches to the Modelling of COVID-19. *Trends in Computational and Applied Mathematics*, **22** (2021), 515–531.

[15] J. Ndam. Mathematical modelling of the dynamics of COVID-19 pandemic. *Asia-Pacific Journal of Mathematics*, **8**(12) (2021), 1–17.

[16] M.B. Neiva, I. Carvalho, E.d.S. Costa Filho, F. Barbosa-Junior, F.A. Bernardi, T.L.M. Sanches, L.L.d. Oliveira, V.C. Lima, N.S.B. Miyoshi & D. Alves. Brazil: the emerging epicenter of COVID-19 pandemic. *Revista da Sociedade Brasileira de Medicina Tropical*, **53** (2020).

[17] Vacinômetro. Vacinômetro-Min.Saúde COVID-19 (2021). URL `https://infoms.saude.gov.br/extensions/SEIDIGI_DEMAS_Vacina_C19/SEIDIGI_DEMAS_Vacina_C19.html`. Acessado em 02/06/2023.

[18] P. Van den Driessche & J. Watmough. Reproduction numbers and sub-threshold endemic equilibria for compartmental models of disease transmission. *Mathematical biosciences*, **180**(1-2) (2002), 29–48.

[19] S. Wiggins. "Introduction to applied nonlinear dynamical systems and chaos", volume 2. Springer (2003).

[20] Worldometer. World / Countries / Brazil: Coronavirus Statistics. Online (2020). URL `https://www.worldometers.info/coronavirus/country/brazil/`. Acessado em 28/02/2023.

How to cite

R. S. Marcolino & J.F.C.A. Meyer. An Application of Two Models for COVID-19 in Brazil. *Trends in Computational and Applied Mathematics*, **26**(2025), e01839. doi: 10.5540/tcam.2025.026.e01839.